10-1-2012

Controlled Spatial Switching and Routing of Surface Plasmons in Designed Single-Crystalline Gold Nanostructures

Rolf Könenkamp
Portland State University, rkoe@pdx.edu

Robert Campbell Word
Portland State University

Joseph Fitzgerald
Portland State University

Athavan Nadarajah

S. D. Saliba
Portland State University

Citation Details

Könenkamp, R. R., Word, R. C., Fitzgerald, J. J., Nadarajah, A., & Saliba, S. S. (2012). Controlled spatial switching and routing of surface plasmons in designed single-crystalline gold nanostructures. Applied Physics Letters, 101(14), 141114.

Controlled spatial switching and routing of surface plasmons in designed single-crystalline gold nanostructures

R. Könenkamp, R. C. Word, J. P. S. Fitzgerald, Athavan Nadarajah, and S. D. Saliba
Physics Department, Portland State University, 1719 SW 10th Avenue, Portland, Oregon 97201, USA

(Received 20 July 2012; accepted 19 September 2012; published online 4 October 2012; corrected 11 October 2012)

Electron emission microscopy is used to visualize plasmonic routing in gold nano-structures. We show that in single-crystalline gold structures reliable routing can be achieved with polarization switching. The routing is due to the polarization dependence of the photon-to-plasmon coupling, which controls the mode distribution in the plasmonic gold film. We use specifically designed, single-crystalline planar structures. In these structures, the plasmon propagation length is sufficiently large such that significant plasmon power can be delivered to the near-field region around the end tips of the router. Solid state devices based on internal electron excitation and emission processes appear feasible. © *2012 American Institute of Physics*. [http://dx.doi.org/10.1063/1.4757125]

Spatial control over plasmon generation and propagation in wave-guide assemblies is currently considered an important step on the research agenda towards plasmonic devices. It has already been shown that plasmon generation can be enhanced and manipulated in antenna structures.[1–3] Devices for controlling plasmon propagation have been demonstrated in the form of beam-splitters[4,5] focusing lenses,[6] and routers and multiplexers.[7] It is believed that the exploration of these basic device functions is needed for the realization of numerous applications ranging from ultra-sensing[8–11] and nanolasing[12,13] to cloaking[14,15] and imaging.[16,17] Optical control is desirable for some of these applications and is essential for high speed transfer of plasmonic signals, energy, or charge. A recent study[7] showed that crossed nanowires selected from a random assembly of single-crystalline nanowires could effectively function as routers or beam splitters. In this case, the nanowires were typically 5–10 μm long and the nanoscale interwire junction region was found to be central for the performance of the wire. When a finite-size gap between the two nanowires existed, the routing effect could be attributed to plasmonic interference at this junction. Depending on the details of gap width, wavelength, and polarization, various routing and multiplexing characteristics could be established.

In this paper, we report efficient routing of surface plasmons in controllably designed planar gold nano-structures of sub-micron size. The routers are carved out of single-crystalline gold platelets using a focused ion beam. The structures consist of gap-less Y-shaped gold platelets with a feature size of ~500 nm. The route switching is due to the polarization dependent in-coupling of light at the external edges of the nanostructures. We use electron emission microscopy to directly visualize the in- and out-coupling of the excitation light. The spatial surface plasmon distribution in the gold is probed with photon energies of 3.1 eV in a non-linear 2-quanta process, while the near-field vicinity of the gold nanostructure is visualized at photon energies of 1.59 eV in a 3-quanta emission process from indium-tin-oxide (ITO). The near-field results illustrate that the plasmon propagation length in these structures is sufficiently large such that significant energy can effectively be routed to specific locations in and outside these structures by switching the polarization state of the excitation light.

Single-crystalline gold platelets were obtained from an aqueous gold-chloride solution with aniline acting as a growth modifier as described in more detail in Refs. 18 and 19. All compounds were analytical pure agents purchased from Sigma Aldrich. 50 ml of ethylene glycol solution containing 0.036 mM $HAuCl_4 \cdot 4H_2O$ was heated to 95 °C for 20 min. Then, 0.1 M aniline solution in ethylene glycol was added under mild stirring to obtain a 2:1 molar ratio of aniline to gold. After 24 h, a variety of gold flakes and platelets with diameters between 3 and 15 μm and thickness between 50 and 100 nm were obtained. These particles were filtered out and then cast on ITO-covered glass-substrates. Figure 1(a) shows examples of the as-prepared single-crystalline platelets on the ITO film. The platelets were then ion-milled to prepare various router structures using a FEI DB237 focused ion beam. The selected platelets were large enough to accommodate 10–20 nanostructures.

An aberration-corrected photoemission electron microscope[20] was used for a direct visual analysis of the plasmon propagation through these designed nanostructures. A mode-locked Ti:sapphire laser provided 100 fs pulses at wavelengths of 780 nm and 410 nm at a repetition rate of 80 MHz. The illumination of the Y-shaped structures occurred at an angle of 60° from the sample normal in the symmetry plane of the Y, as illustrated in Figure 1(b). The polarization of the excitation light was switched between +45° and −45° from the p-polarization plane using a tunable waveplate.

On the basis of earlier work on non-linear photoelectron emission in a similar configuration,[21] the excitation process is thought to involve the following steps: Femtosecond pulses at the chosen wavelength are absorbed in the gold film exciting surface plasmon polaritons—predominantly with the same quantum energy as the exciting photons. As the intensity within the femtosecond pulses is high, there is, however, a sizeable probability for non-linear excitations, and therefore plasmons with doubled, tripled, and possibly higher quantum energies are also excited. These coherently

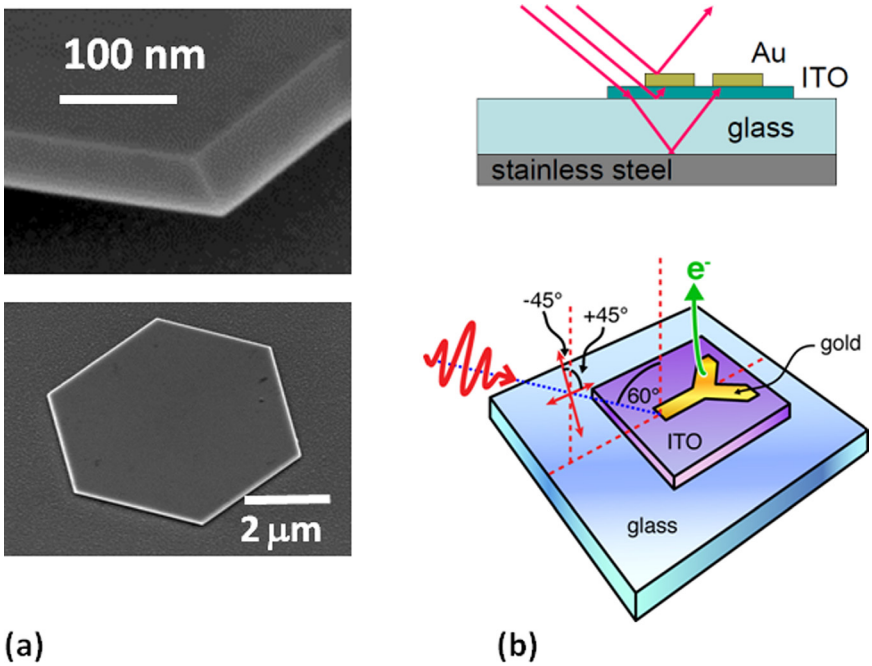

FIG. 1. (a) Scanning electron micrographs of as-prepared single-crystalline gold platelets showing typical size, geometry, and thickness; (b) illumination scheme in the emission microscope showing sample structure and orientation.

excited higher order collective excitations are thought to provide the energy needed for single-electron excitations beyond the work-function barrier, such that electron emission from the gold is observed. Reference 21 also shows evidence against the alternate possibility that the electron emission from the gold originates directly from multi-photon excitations. In our earlier work,[22,23] we observed electron emission from material outside the gold film, but within the near-field region of the gold. Essentially, the gold films are found to act as plasmonic receivers, inducing electron emission in adjacent ITO regions whose workfunction is substantially lower than that of gold. For this near-field emission it is currently not known, if it involves a decay of surface plasmons into photons prior to the observed electron emission, or if the emission energy is also of plasmonic nature. Once emitted, the electrons are accelerated to 20 keV and then imaged in the microscope.

In this paper, we show results obtained at two different photon energies, 3.1 and 1.6 eV, corresponding to wavelengths of 410 nm and 780 nm, respectively. We observe electron emission in a 2-quanta-process from gold using a photon energy of 3.1 eV. At photon energies of 1.6 eV, we observe electron emission in a 3-quanta-process from ITO in the near-field region of the gold structure. These observations are well explained by assuming that the work function of the gold surface is typically >5.0 eV, while it is approximately 4.3 to 4.7 eV for ITO in practical work involving ultraviolet light.[24,25] In that case, both materials require a two-quanta emission process for 3.1 eV photon energies, but the gold surface with its higher electron density will be dominating in the emission images and, on a linear scale, hardly any emission from the ITO will be apparent. For 1.6 eV photon energies, emission from gold requires a 4-quanta process, while for emission from ITO a 3-quanta process is sufficient. In this case, the emission from the ITO turns out to be dominant. This is likely due to the much reduced probability for the 4-quanta process. Thus, by varying the excitation energies we can select the imaging of different processes: electron emission from the near-field vicinity outside the plasmon excited metal structures and emission from the plasmonically active metal region itself. More experimental details are given in Ref. 23.

In Fig. 2, we show experimental results obtained at a wavelength of 410 nm, i.e., 3.1 eV. Here, the excited gold surface is imaged. The micrographs in (a) show two superimposed electron emission images obtained under illumination with +45° and −45° polarizations. Electron emission from light with a polarization angle of +45° is colored in green, electron emission from light with −45° polarization is colored in red. The brightness scales with the electron emission rate. It is seen that the emission rate is distributed quite differently for the two light polarizations. This apparently results from a polarization-dependent in-coupling of the optical power: The in-coupling of light is most efficient at the edge of the Y structure, where the light polarization vector can have a large component perpendicular to the metal surface. This is the case along the left edge of the Y for a polarization of −45° and along the right edge at a polarization of +45°. These observations are consistent for the whole set of samples ranging in size from 400 nm to 2 μm. As shown in parts (c) and (d) of the figure, the contrast for the two polarizations is approximately 2, i.e., for a given polarization the average electron emission rate differs by approximately a factor 2 between the two edges. The micrographs thus indicate a fairly high selectivity for the polarization direction based on the in-coupling process.

Next, we show that sufficient plasmonic energy can be transported to the two tips of the Y-structures and coupled into the near-field region outside the plasmonic router. As discussed above, electron emission in the near-field region can be studied at photon energies of 1.6 eV in 3-quanta processes originating from the ITO, which dominates over 4-quanta emission from the gold surface. Fig. 3 shows that for a given polarization there occurs strong localized emission at the periphery of the Y, and typically one of the two upper legs of the Y. For example, as shown in part (b) of the figure,

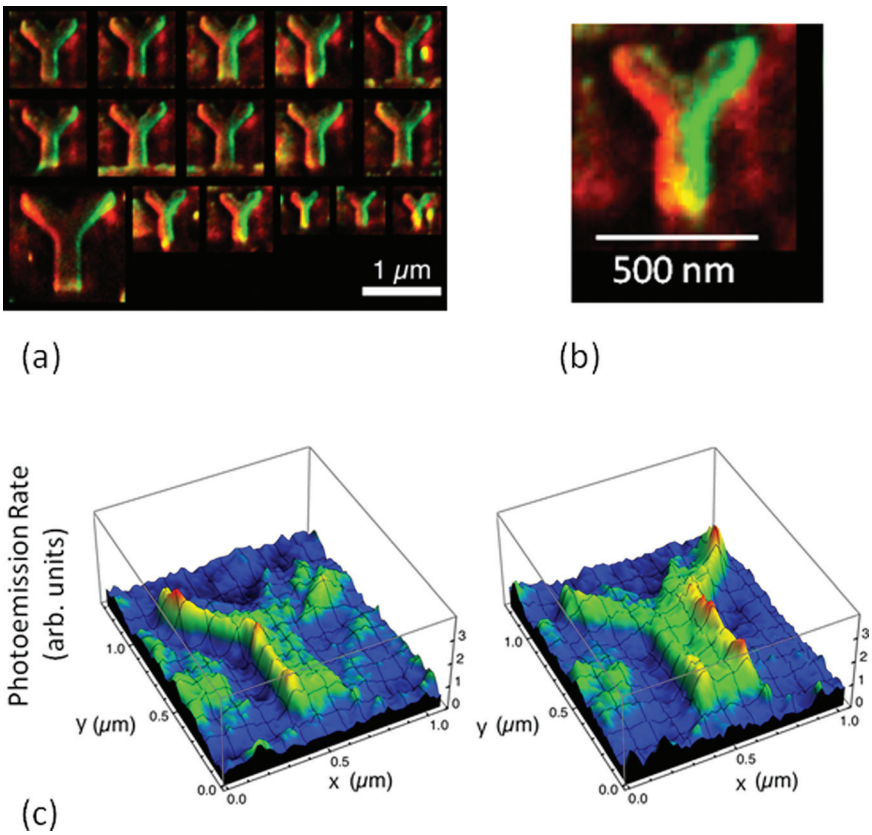

FIG. 2. (a) False color composite image of two PEEM micrographs taken with +45° and −45° polarizations; green brightness represents electron emission rate obtained for +45° polarization, red brightness represents electron emission obtained for −45° polarization. (b) Details of a structure from part (a). (c) Emission rate distribution for −45° polarization (left) and +45° polarization (right).

for polarization at −45° the right upper leg of the Y structures shows strong emission, while the left tip region is essentially dark. In this case, the emission on the right is ∼20 times than the emission intensity on the left end. Similarly for +45° polarization, enhanced emission at the left upper leg is predominantly observed. The results indicate that the plasmon propagation length in these structures is sufficient to deliver a significant amount of energy to the top legs of the Y structure and towards the edge opposite to the in-coupling region.

The emission for 780 nm excitation shows all the characteristics of localized plasmon hot spots originating from ITO as discussed above and in an earlier paper:[23] The emission area diameter is of the order of 50 nm, the emission rate has a 3rd order power dependence, and the energy threshold is consistent with the work-function of the ITO. It is noted

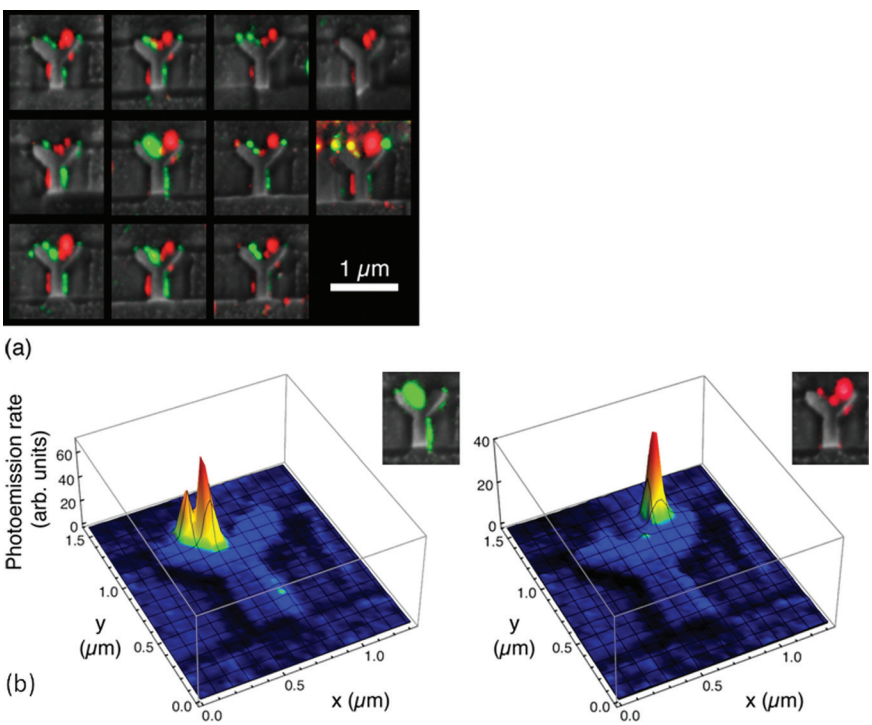

FIG. 3. (a) Eleven routers carved from a triangular gold platelet. Composite PEEM images obtained with dc-illumination at 244 nm from a frequency-doubled Ar^+ laser (gray scale) and pulse illumination at 780 nm (color). Electron emission for −45° polarization is represented in red, for +45° electron emission is in green. Hot spots at the end points of the Y structure are clearly seen indicating polarization-selective emission from ITO. No emission from the front edge or the surface of the Y-structure is seen. (b) Digital plot of the emission rate for −45° degree polarization. This image is obtained with simultaneous illumination from a Hg lamp to provide the contour of the Y structure, and laser pulses at 780 nm for the plasmon excitation. When the emission from the Hg lamp is taken into account, the brightness ratio between the right and left-hand tips of the Y is found to be >10.

that only weak emission is observed at the bottom edge of the Y structures, consistent with the understanding that the plasmon propagation direction is in the forward direction of the exciting illumination, and that only a small portion of the plasmon energy is reflected back to the base region of the Y. The 11 monolithic structures shown in Fig. 3(a) again show good reliability in the polarization selectivity. While there is some weak emission at most edges of the structure, the predominant emission always occurs near the upper legs of the Y, and for $+45°$ polarization this emission is centered on the left, while of $-45°$ polarization it is centered on the right.

It can be expected that with improved fabrication of the structures, the emission areas can be better defined and the emission process be made more efficient. An estimate of the current emission rates from the localized hot spots indicates that they are much lower than one electron per light pulse. An increase in emission rates could be expected when the pulse power is raised, i.e., with shorter or more focused pulses, or when more emissive materials are chosen, or when lower-order, possibly linear, excitation schemes are used. While the present work was based on external electron emission, similar devices could also be designed on the basis of internal emission processes, where a bound excited state inside the device material or within its near-field region is prepared. In this case, the excited electrons could subsequently contribute to photoconductance, luminescence, or charge transfer in a solid-state routing device.

To conclude, photoemission electron microscopy has been used to directly visualize plasmonic routing. Energy and charge deliverance to the endpoints of designed single-crystalline gold nano-structures has been demonstrated. Using polarization switching, reliable routing was performed. The energy transfer within the submicron routers is sufficient to allow non-linear electron emission processes. Structures with lateral size of 400 nm were effective in the routing process. In these first-generation structures, the electron emission rates are low, but higher rates appear feasible. Alternative devices based on internal excitation processes rather than excitation to the vacuum, appear feasible.

This research was funded by the US Department of Energy Basic Science Office under Contract No. DE-FG02-10ER46406.

[1]A. V. Akimov, A. Mukherjee, C. L. Yu, D. E. Chang, A. S. Zibrov, P. R. Hemmer, H. Park, and M. D. Lukin, Nature **450**, 402 (2007).
[2]M. W. Knight, N. K. Grady, R. Bardhan, F. Hao, P. Nordlander, and N. J. Halas, Nano Lett. **7**, 2346 (2007).
[3]H. Wei, D. Ratchford, X. Q. Li, H. X. Xu, and C. K. Shih, Nano Lett. **9**, 4168 (2009).
[4]A. B. Evlyukhin, S. I. Bozhevolnyi, A. L. Stepanov, and J. R. Krenn, Appl. Phys. B. **84**, 29 (2006).
[5]C. Tai, S. H. Chang, and T. J. Chiu, Opt. Soc. Am. **25**, 1387 (2008).
[6]Z. Liu, J. M. Steele, W. Srituravanich, Y. Pikus, C. Sun, and X. Zhang, Nano Lett. **5**, 1726 (2005).
[7]Y. Fang, Z. Li, Y. Huang, S. Zhang, P. Nordlander, N. J. Halas, and H. Xu, Nano Lett. **10**, 1950 (2010).
[8]Z. Y. Li and Y. N. Xia, Nano Lett. **10**, 243 (2010).
[9]Z. Zhang, A. Weber-Bargioni, S. W. Wu, S. Dhuey, S. Cabrini, and P. J. Schuck, Nano Lett. **9**, 4505 (2009).
[10]Y. R. Fang, H. Wei, F. Hao, P. Nordlander, and H. X. Xu, Nano Lett. **9**, 2049 (2009).
[11]H. X. Xu, E. J. Bjerneld, M. Kall, and L. Borjesson, Phys. Rev. Lett. **83**, 4357 (1999).
[12]M. A. Noginov, G. Zhu, A. M. Belgrave, R. Bakker, V. M. Shalaev, E. E. Narimanov, S. Stout, E. Herz, T. Suteewong, and U. Wiesner, Nature **460**, 1110 (2009).
[13]S. Lal, S. E. Clare, and N. J. Halas, Acc. Chem. Res. **41**, 1842 (2008).
[14]N. Fang, H. Lee, C. Sun, and X. Zhang, Science **308**, 534 (2005).
[15]A. Alu and N. Engheta, Phys. Rev. Lett. **100**, 113901 (2008).
[16]I. I. Smolyaninov, Y. J. Hung, and C. D. Christopher, Science **315**, 1699 (2007).
[17]Z. W. Liu, H. Lee, Y. Xiong, C. Sun, and X. Zhang, Science **315**, 1686 (2007).
[18]Z. Guoa, Y. Zhang, Y. D. Mu, L. Xu, S. Xie, and N. Gua, Colloids Surf., A **278**, 33 (2006).
[19]J. Huang, V. Callegari, P. Geisler, C. Brüning, J. Kern, J. C. Prangsma, X. Wu, T. Feichtner, J. Ziegler, P. Weinmann, M. Kamp, A. Forchel, P. Biagioni, U. Sennhauser, and B. Hecht, Nature Commun. **1**, 150 (2010).
[20]R. Könenkamp, R. C. Word, G. F. Rempfer, T. Dixon, L. Almaraz, and T. Jones, Ultramicroscopy **110**, 899 (2010).
[21]M. Merschdorf, W. Pfeiffer, A. Thon, S. Voll, and G. Gerber, Appl. Phys. A **71**, 547 (2000).
[22]R. C. Word, J. Fitzgerald, and R. Könenkamp, Appl. Phys. Lett. **99**, 041106 (2011).
[23]R. C. Word, T. Dornan, and R. Könenkamp, Appl. Phys. Lett. **96**, 251110 (2010).
[24]K. Sugiyama, H. Ishii, Y. Ouchi, and K. Seki, J. Appl. Phys. **87**, 295 (2000).
[25]J. S. Kim, B. Lagel, E. Moons, N. Johansson, I. D. Baikie, W. R. Salaneck, R. H. Friend, and F. Cacialli, Synth. Met. **111–112**, 311 (2000).